Applied Catalysis B: Environmental 186 (2016) 10–18

Contents lists available at ScienceDirect

Applied Catalysis B: Environmental

journal homepage: www.elsevier.com/locate/apcatb

Innovative CVD synthesis of Cu_2O catalysts for CO oxidation

Achraf El Kasmi[a,b], Zhen-Yu Tian[b,d,*], Henning Vieker[c,e], André Beyer[c], Tarik Chafik[a,*]

[a] Laboratory LGCVR, Faculty of Sciences and Techniques, University Abdelmalek Essaadi, B.P. 416 Tangier, Morocco
[b] Department of Chemistry, Bielefeld University, Universitätsstraße 25, D-33615 Bielefeld, Germany
[c] Department of Physics, Bielefeld University, Universitätsstraße 25, D-33615 Bielefeld, Germany
[d] Institute of Engineering Thermophysics, Chinese Academy of Sciences, 100190 Beijing, China
[e] Present address: CNM Technologies GmbH, 33609 Bielefeld, Germany

ARTICLE INFO

Article history:
Received 10 September 2015
Received in revised form
11 December 2015
Accepted 18 December 2015
Available online 29 December 2015

Keywords:
Catalytic oxidation
Carbon monoxide
Water effect
Pulsed-spray evaporation
Chemical vapor deposition

ABSTRACT

The present work reports on a one-step synthesis of thin Cu_2O films deposited at 250 °C using pulsed-spray evaporation chemical vapor deposition (PSE-CVD). Of interest, water addition (0, 2.5 and 5 vol.%) in the liquid feedstock of $Cu(acac)_2$ and ethanol was found to have a significant effect on the catalytic performance of these films towards CO oxidation. The obtained films were comprehensively characterized with X-ray diffraction (XRD), Helium ion microscopy (HIM), X-ray photoelectron spectroscopy (XPS) and Ultraviolet–visible (UV–vis) spectrometry. Both the surface composition and optical properties exhibited good correlation with the catalytic activity. The adopted empirical catalytic screening based on light-off curves measurement demonstrated that Cu_2O prepared with 5 vol.% of water in the reactant feedstock exhibited the best performance with respect to complete oxidation of CO at 175 °C. This finding is reproducible and tentatively attributed to reduced crystallite grain size and more surface oxygen species generated when water was added in the feedstock. Accordingly, the innovative combination of water addition in the feedstock and the use of PSE-CVD technique is expected to assist further synthesis of new efficient thin films paving the way for catalytic applications.

1. Introduction

Cuprous oxide (Cu_2O) presents major interesting characteristics: it is not toxic, abundantly available, not costly and environmentally friendly [1]. Due to its fascinating properties [2,3], Cu_2O is useful in a wide range of applications such as solar energy conversion [2,4], lithium ion batteries [5,6], gas sensors [7,8], photocatalysis for splitting water into O_2 and H_2 under visible light [9–14] and degradation of organic pollutants under visible light irradiation [15], catalytic oxidation [16] and complete CO oxidation [17]. Different methods have been used to synthesize Cu_2O as a nanostructured material including thermal oxidation of Cu metal [18], spray pyrolysis deposition [19], solvothermal synthesis [20], solution-phase reduction [21], thermal decomposition [17,22], electro-deposition [23,9], sol–gel-like dipping [24], magnetron sputtering [25], microplasma method [26] and chemical deposition [27–29]. In most of these studies, a mixture of Cu, CuO and Cu_2O was generally obtained. However, it was reported that the Cu_2O films could be formed at low deposition temperature (200–250 °C) [30], while at higher temperature the Cu_2O could easily convert to the CuO phase [18,29,30]. Moreover, Cu_2O was mostly prepared by an indirect strategy using either reducing agents [21,31] or surfactants [21,32]. In spite of its promising material properties, the direct synthesis of pure Cu_2O is scarce.

Pulsed-spray evaporation chemical vapor deposition (PSE-CVD) has been used before in the tailored synthesis of thin films of different metals [33,34] and oxides [35–40]. PSE-CVD is a facile, direct and inexpensive technique for the preparation of continuous thin film oxides on a variety of substrates without any after-treatment. It offers potential for producing films with high uniformity of thickness, high purity, conformal step coverage, minimal substrate damage, the possibility of growth in selected area and the flexibility to use different precursors in the feedstock simultaneously. This latter capacity allows using multiple precursors in a liquid feedstock providing a rationally controllable route for the growth of functional oxides [35,38–40]. PSE-CVD was thus selected here for the synthesis of pure Cu_2O, intended for low-temperature CO oxidation.

The complete oxidation of CO is an important target in view of increasingly strict environmental regulations within an economical way [41,42,17]. This issue is also targeted in the field of

* Corresponding author. Fax: +86 10 82543184.
E-mail addresses: tianzhenyu@iet.cn (Z.-Y. Tian), t.chafik@fstt.ac.ma, /tchafik@yahoo.com (T. Chafik).

http://dx.doi.org/10.1016/j.apcatb.2015.12.034
0926-3373/

H_2-production as an energy source for fuel cells [43,44], because trace amount of CO can poison a fuel cell electrode and thus drastically reduce its efficiency [45–47]. Low-temperature catalytic oxidation of CO is thus becoming increasingly important in terms of cleaning air and lowering automotive emissions with cheap and efficient air pollution technology [48–50].

Precious metals were normally used as the efficient catalysts for CO oxidation with high activity and stability [42,50,51]. This reaction was also reported to be achieved over noble metal nanoparticulates supported on transition metal oxides (TMOs) [52–57]. However, due to the high price, limited resources and tendency to poisoning of precious metals, considerable attention has been paid to develop catalysts based on transition metals such as cobalt- [48,58], manganese- [37], iron- [36] and copper-based oxides [30,59] as well as their mixed oxides for CO oxidation [60,61] regarding their competitive activity, easy manufacturing, high thermal stability and low cost.

The present study aims to highlight an innovative approach to synthesize catalytically active pure Cu_2O thin films using a direct PSE-CVD strategy. Particular attention was paid to investigation of the effect of water addition in the precursor feedstock using an empirical method based on catalytic performance screening. An attempt was made so as to reveal the relationship among the water effect, structure, morphology, optical properties and chemical composition of the prepared films. Accordingly, a possible mechanism was proposed for CO oxidation over the prepared Cu_2O thin films paving the way for catalytic applications. To the best of our knowledge this issue has never been addressed before.

2. Experimental

2.1. Preparation

The synthesis of Cu_2O thin films was carried out in a cold-wall stagnation point-flow CVD reactor employing a PSE unit for the delivery of liquid precursor feedstock [33,58]. In the deposition process, commercially available $Cu(acac)_2$ (Merck, 99%) was used as precursor and dissolved in ethanol, then different amounts of deionization water (vol. 0%, 2.5% and 5%) were added into the feedstock. When vol. 10% of water is added into the feedstock, the complete dissolution of the precursor cannot be achieved. The PSE delivery of the feedstock was achieved using a four-pinholes injector (Bosch) with a frequency of 4 Hz and a valve opening time of 7 ms. The feedstock, with a feeding rate of 0.83 ml/min, was injected as a fine spray into a 30 cm long evaporation chamber kept at 180 °C. The resulting vapor was transported to the deposition chamber kept at 200 °C, with N_2/O_2 flow rates of 0.5/1.0 standard liter per minute (slm) under a total pressure in the reactor of 24 mbar. During the deposition process, planar glass, silicon, stainless steel plates and mesh grid (stainless steel, SPW 40, 80 × 400, micrometer retention 36–45 μm) were used as substrates and were heated to 250 °C using a flat resistive heater. These substrates were selected to meet the requirements of the different characterization techniques. The experimental conditions for the preparation are shown in Table S1. The thickness of the deposited films was estimated gravimetrically by measuring the weight change of the substrates with a microbalance (Mettler ME30, digital resolution of 1 μg). The obtained films from vol. 0%, 2.5% and 5% in the feedstock are marked with Cu_2O 0%, Cu_2O 2.5% and Cu_2O 5%, respectively.

2.2. Characterization

The identification of the crystalline phases of the deposited films was identified by XRD using a Phillips X'Pert Pro MDR equipped with a Cu Kα (λ = 0.154056 nm) radiation source and operated at 40 kV and 30 mA. Data were recorded in the 2θ range from 20° to 80°, with a step size of 0.05°. XRD was carried out under ambient conditions. The crystalline phases were identified by referring to the powder XRD database (JCPDS-ICDD). The surface morphology of the obtained films was examined by HIM (Carl Zeiss Orion Plus® instrument). The helium ion beam was operated at an acceleration voltage of 36 kV and a current between 0.3 and 1.7 pA and a 10 μm Aperture at Spot Control 4 to 5. Secondary electrons were collected by an Everhart–Thornley detector at 500 V grid voltage. The samples were plasma-cleaned in the HIM Load-Lock for 8 min before measurement.

The film composition was determined by XPS (Multiprobe, Omicron Nanotechnology) in a multi-technique UHV instrument (base pressure is 5×10^{-10} mbar) using a monochromatic Al Kα X-ray source (1486.7 eV, 270 W) under an angle of 13° from the surface normal to the electron detector. CasaXPS was used for the analysis of the XPS spectra, using Scofield photoionization cross-sections and a Shirley background subtraction procedure. The optical band gap energies of the deposited samples were assessed using a Shimadzu UV-2501 PC UV–vis spectrometer at room temperature.

2.3. Catalytic test

The catalytic performance of the Cu_2O samples was evaluated at atmospheric pressure using a quartz plug-flow reactor (9.0 mm inner diameter) with 15 mg catalyst grown on mesh grid of stainless steel. Blank experiments were performed using a reactor filled with non-coated mesh of stainless steel. The reaction gas mixture consisted of 1% CO and 10% O_2 diluted in argon with a total flow rate of 15 ml/min, corresponding to a weight hourly space velocity (WHSV) of 60000 ml g^{-1}_{cat} h^{-1}. The flow rates of gases were controlled by MKS mass flow controllers and the temperature of the reactor was raised with a ramp of 5 °C/min using a HT60 controller (Horst). The temperature of the mesh inside of the reactor was recorded using K-type thermocouples and a digital thermometer (GMH3250, Greisinger). The composition of the effluent gas at the outlet was detected in the wavelength range of 400–4000 cm^{-1} with an online FTIR spectrometer (Nicolet FTIR 5700) equipped with a KBr transmission cell. Details of data treatment can be found elsewhere [62]. To prevent collapse of the tested catalysts [29,30], the tests were carefully carried out in a temperature regime at which the Cu_2O structure survives for several turns.

3. Results and discussion

3.1. Structure

XRD analysis was performed to investigate the crystalline structure and the purity of the thin films deposited at 250 °C. The XRD patterns of the thin films coated on glass obtained using different water content are presented in Fig. 1a. The diffraction peaks of the as-deposited films are observed at 2θ of 29.55°, 36.42°, 42.30°, 61.34° and 73.52°, corresponding to (1 1 0), (1 1 1), (2 0 0), (2 2 0) and (3 1 1) orientations of Cu_2O in the literature. All peaks fit well with the cubic structure of Cu_2O (JCPDS No. 05-0667), indicating that a pure Cu_2O was readily synthesized. It is worth to point out that the formed structure is insensitive to the amount of water added in the feedstock (vol. 0%, 2.5% and 5%). The XRD patterns show no peaks of impurity phases, which reveals the high purity of the all deposited films. It should be mentioned that the increase in the amount of water added in the feedstock up to 10% also results in the same crystalline structure (see Fig. S1). However, the precursor was observed to be incompletely dissolved in the liquid feedstock with vol. 10% water, which prohibits this sample from further test in this work.

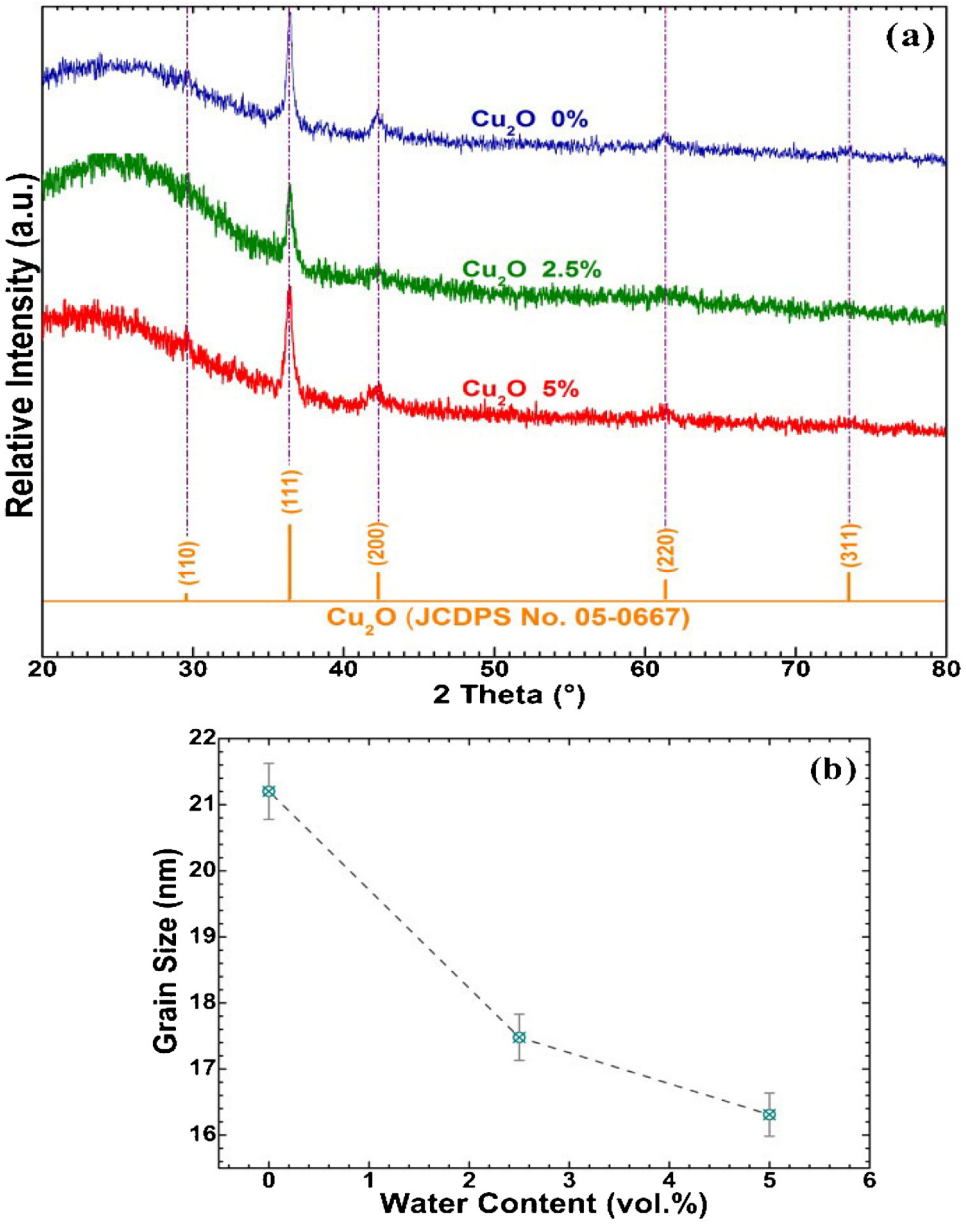

Fig. 1. XRD patterns of Cu_2O thin films (a) and derived variation of grain size as a function of the water content in the liquid feedstock (b).

The presence of the strongest peak at $2\theta = 36.42^\circ$ demonstrates that the (1 1 1) plane is the preferred growth direction within the Cu_2O cubic structure. By applying the Debye–Scherrer equation, $D = 0.9\lambda/\beta\cos\theta$, where $\lambda = 0.154056$ nm, θ is the Bragg angle and β is the full width at half maximum of the strongest peak, the crystallite sizes were calculated, as shown in Fig. 1 b. The crystallite size of the deposited films tends to decrease when the water content was increased in the feedstock, which reflects a synergistic effect of added-water during deposition process.

Several studies reported the formation of Cu_2O prepared by using reducing agents [21,31] or surfactants [21,32]. Here we could demonstrate that synthesis of Cu_2O films without any reducing agents or surfactants also leads to nanocrystalline structure. It was reported before that the catalytic activity increases with decreasing the particle size [63]. Furthermore, the small grain size is also known to have a beneficial effect on active sites dispersion and it would be necessary to increase the efficiency of the catalytic performance [64,65]. In this regard, the small grain size can be easily

Table 1
Surface composition of Cu_2O samples.

	O/Cu(at.ratio)	$O_{Lattice}$/Cu(at.ratio)	$O_{Adsorbed}$ (%)		$O_{Lattice}$
			H_2O/organic	OH^-/def./organic	
Cu_2O 0%	1.8	0.9	3.7	48.3	48.1
Cu_2O 2.5%	2.1	0.9	12.4	46.1	41.5
Cu_2O 5%	2.7	1.0	12.0	49.8	38.3

controlled here with high water content in the liquid feedstock, which would further benefit the catalytic reaction Table 1.

3.2. Morphology

To investigate the surface morphology of the deposited films, Helium ion microscopy (HIM, Carl Zeiss Orion Plus® instrument), a recently developed imaging technique similar to scanning electron microscopy was used in the present work [66]. The helium ion beam can be focused into a smaller probe size and provides a much smaller interaction volume at the sample surface than in typical electron microscopy, allowing HIM the possibility to achieve higher contrast and improved surface sensitivity. Thus it is possible to obtain superior resolution and depth of field. Fig. 2 shows the HIM images of representative Cu_2O thin films. The images obtained from HIM at low resolution (Fig. 2a–c) show no significant difference between samples deposited with different water content. Moreover, all films show an open and porous structure, expected to provide predisposed space holding numerous active sites. The agglomeration of quite uniform nanocrystals is seen from Fig. 2d–f. These nanocrystals are visible in more detail from Fig. 2g–i as small grains embedded in a matrix. Interestingly, those obtained without water in the feedstock show a much more defined crystal structure. With the addition of water, the grains appear to lose their defined shape, which may result from the decrease in grain size, as revealed by the XRD analysis. The observed decrease in the particle size may be due to the generated species during deposition process followed by adsorption on crystals' surfaces [67], which in turn, leads to much small particles structure, presumably because the nanocrystal structure size is thermodynamically more stable under the current synthetic conditions. Nevertheless, the relatively loose surface structure may involve oxygen vacancies, which would further benefit its catalytic performance.

3.3. Chemical composition

The surface chemical composition of the Cu_2O films was analyzed with ex situ X-ray photoelectron spectroscopy (XPS, Multiprobe, Omicron Nanotechnology) to understand the properties of the catalytically active layer including its oxidation states. The high-resolution XP spectra of Cu 2p and O 1s for all deposited films with different water content in the feedstock are shown in Figs. 3 and 4. The XP spectra of Cu 2p show the presence of two major peaks of Cu $2p_{3/2}$ and Cu $2p_{1/2}$ located at binding energies (BE) of ~934 and ~954 eV, in line with previously reported results [68]. It should be mentioned that the satellite structure at 942 eV and 963 eV comes from copper oxide and a small amount of copper hydroxide. These species could be formed by the reaction of Cu_2O with oxygen at the surface.

The O 1s spectra were deconvoluted into three main components in the BE range of 529–534 eV. The peak located at 530 eV is characteristic of the lattice oxygen species O_2^-, while the peaks at higher binding energies are assigned to the presence of adsorbed species. The peak located at around ~531.4 eV is attributed to the hydroxyl species OH^-, organic oxides or defects in the structure, and the peak at ~533.7 eV can be attributed to adsorbed oxygen species [68,69].

The atomic ratio of O and Cu at the surface of the deposited films increased from ~1.8 for Cu_2O 0% to ~2.1 and ~2.7 for Cu_2O 2.5% and Cu_2O 5%, respectively, as shown in Tables 1 and S2. On

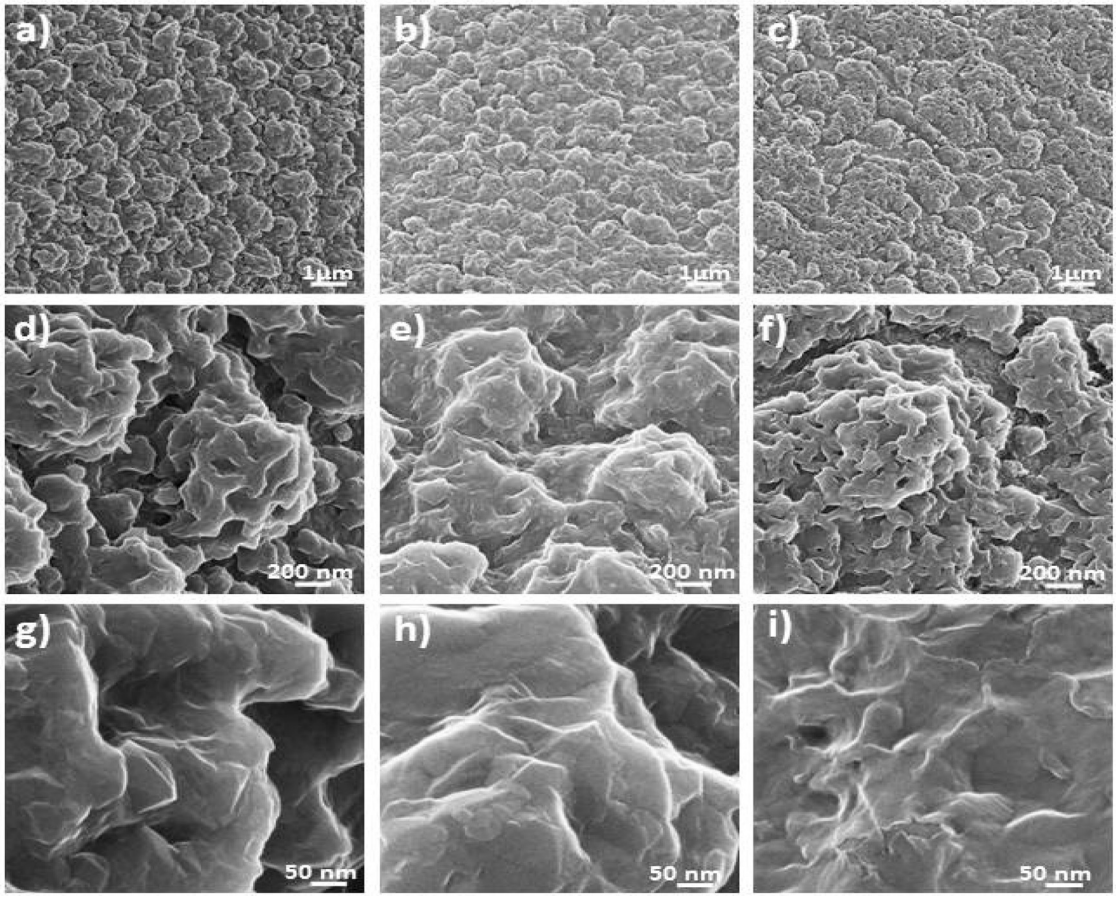

Fig. 2. HIM images of Cu_2O films deposited on bare glass with different water content, 0% (a, d, g), 2.5% (b, e, h) and 5% (c, f, i).

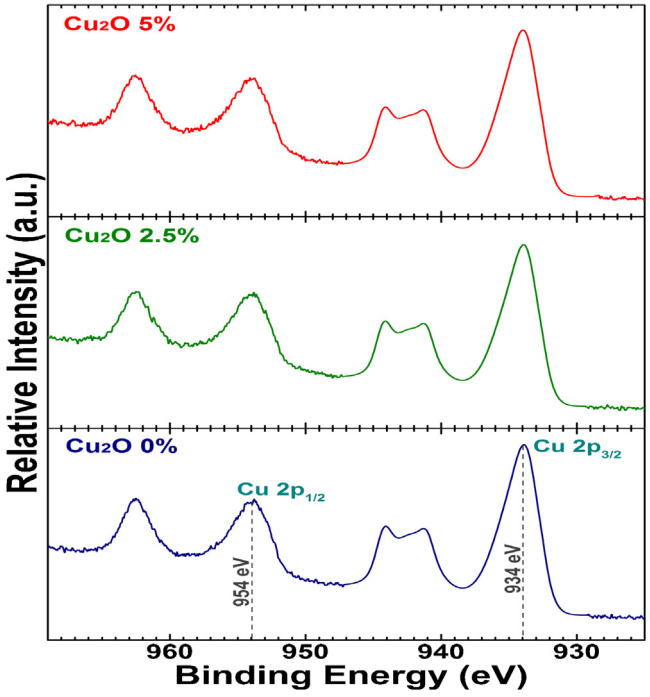

Fig. 3. XP Spectra of Cu 2p for deposited Cu_2O films with different water contents.

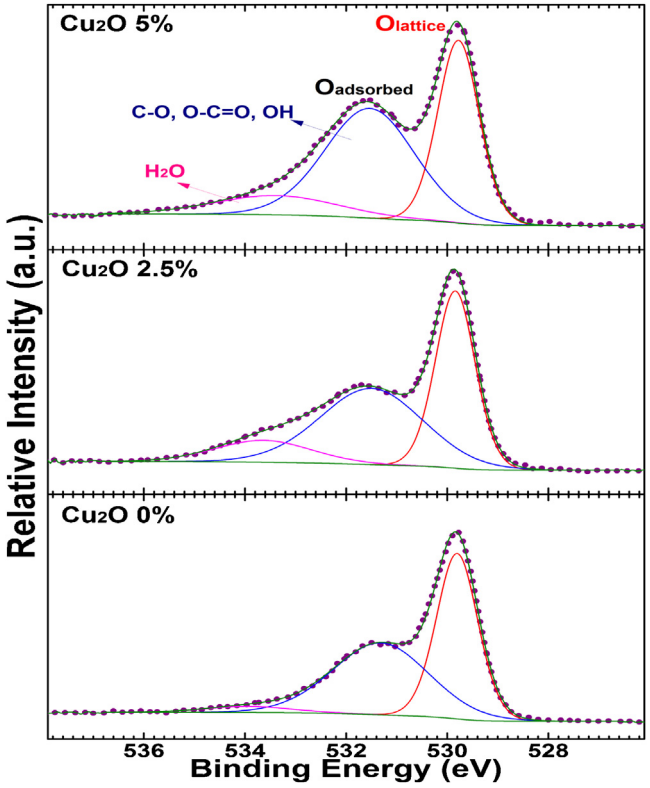

Fig. 4. XP Spectra of O 1s for deposited Cu_2O films with different water contents.

the other hand, the XPS results of all deposited films exhibit the presence of lattice and adsorbed oxygen at the surface (see Fig. 4). Since the ratio of lattice oxygen to copper is ~1 for all samples, as obtained from the XPS analysis on the surface, the variation in the surface oxygen content is due to the difference in the water content in the feedstock as evident in Fig. 4. In line with these observations, Pinkas et al [70]. concluded that the oxygen observed in a film of mixed copper oxide (mainly Cu_2O and a small amount of CuO), deposited by CVD, is derived from water and not from the ligand. In the present work, the O 1s species with high binding energy increases for both samples grown with water. These results reveal an increase in surface oxygen content, which confirms that the water content in the feedstock generate more oxygen species at surface. Thus, the difference in the surface oxygen content of the deposited films is expected to induce different catalytic behaviors with respect to CO oxidation.

3.4. Optical properties

In previous work, the metal oxides with low band gap energy (E_g) were reported to exhibit good performance [71,72]. To determine E_g and to correlate it with the catalytic performance of the catalysts, the UV–vis spectra were measured to investigate the optical properties of the deposited films. E_g in each case was derived from Tauc's equation: $\alpha h\upsilon = A(h\upsilon - E_g)^n$, where α represents the absorption coefficient, hυ is the photon energy, A is the refractive index constant and n is a constant related to the nature of the transition (1/2 for direct allowed transition). The corresponding Tauc plots of $(\alpha h\upsilon)^2$ versus hυ for the Cu_2O films are shown in Fig. 5a. The E_g values of each sample were determined from the intersection of the straight line with the $h\upsilon$-axis [73]. The E_g for the Cu_2O 0% sample is 2.16 ± 0.05 eV, which is consistent with a previously reported value of 2.17 eV [74,75]. Upon increasing the water content in the feedstock by 2.5% and 5%, the values of E_g shift linearly to 2.04 and 1.92 ± 0.05 eV (Fig. 5b), indicating that the water addition could lead to low E_g. Besides, E_g was also reported to decrease with increase in oxygen flow rate during deposition [76]. In the current work, the low E_g with high water content (i.e, high oxygen content) in the feedstock could result from the formation kinetics of the thin films during the deposition process. This finding shows that the optical properties of the deposited films could be controlled by adjusting the feedstock content.

In the literature, it was reported that several factors could affect the E_g of metal oxides: defects, charged impurities, disorder at the grain boundaries etc [77]. Moreover, even a small change in grain size may generate a material with drastically different characteristics [78]. Although the decreases in E_g revealed by pure deposited V_2O_5 thin films was attributed to the increase of the grain size, grain distribution and the structural modification of the material [77], the E_g is found here to decrease with decreasing in the crystallite grain size, whereas the crystalline structure is still unaltered. Moreover, it was reported that there was a strong correlation between E_g and catalytic performance [72]. Consequently, the variation obtained in the E_g accompanied by decreasing in crystallite grain size could result in the difference of the catalytic performance.

3.5. Catalytic performance

Fig. 6 shows the light-off curves corresponding to the temperature-dependent conversion of CO to CO_2 over Cu_2O films obtained with different water contents in the feedstock considering non-coated mesh as reference experiment. The Cu_2O thin film catalyst prepared without water (Cu_2O 0%) in the feedstock shows the lowest activity for CO oxidation starting at around 140 °C and completed at 238 °C. The Cu_2O thin film catalysts prepared by the addition of water yield to gradual enhancement of the catalytic oxidation. For 2.5% of water in feedstock (Cu_2O 2.5%), the oxidation of CO started at 130 °C, and the complete conversion of CO was achieved at 220 °C. For the sample prepared with feedstock containing 5% of water (Cu_2O 5%), a significant decrease is observed of the starting and complete conversion temperatures at 100 and 175 °C, respectively (see Fig. 6). This finding is of interest as compared to the previous published results: for example, the com-

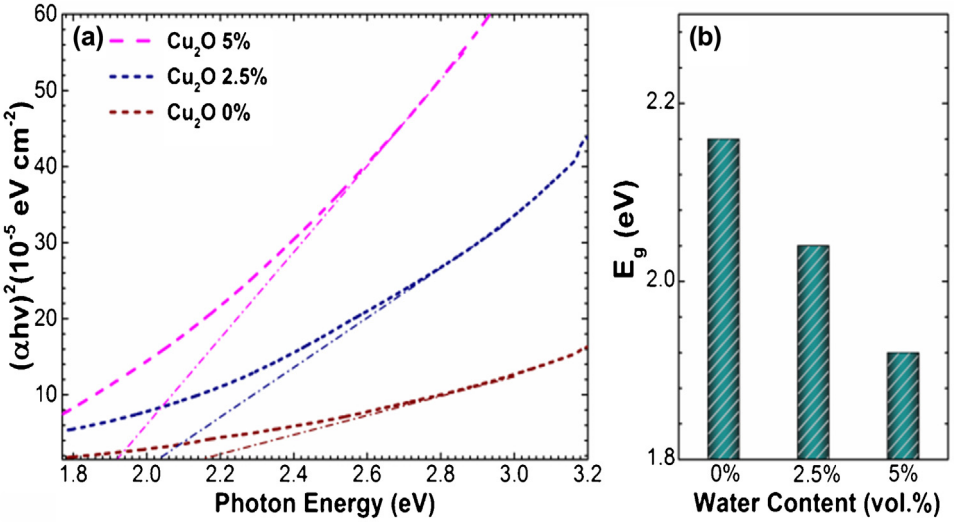

Fig. 5. Tauc's plot for Cu_2O films deposited with different water content (0%, 2.5% and 5%) (a); Variation of optical band gap energy (E_g) of deposit films with different amounts of water in feedstock (b).

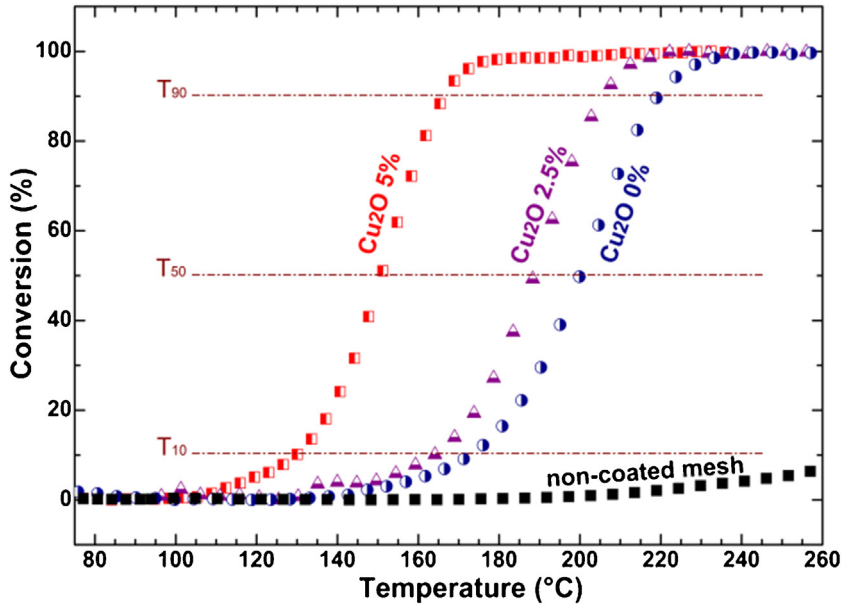

Fig. 6. Light-off curves of CO conversion over Cu_2O coated on the mesh of stainless steel and non-coated mesh.

plete oxidation of CO was achieved at temperatures around 250 °C, regardless the consideration of the difference in WHSV values, over Cu_2O supported on silica gel [17]. In comparison to the catalytic CO oxidation behavior for a number of interesting oxides at different temperatures of T_{10}, T_{50} and T_{90} (temperatures at 10%, 50% and 90% of CO conversion, see Table S3), the Cu_2O samples prepared in the present work are quite promising in terms of activity. The reproductivity of the obtained results was verified by reusing the catalysts for several times and some light-off curves are shown in Fig. S3.

Based on the XRD analysis, the catalytic behavior can be reasonably attributed to the smallest crystallite size observed for Cu_2O 5%. This phenomenon reflects a synergistic effect between the added water and the precursor during the deposition process. According to the literature, the crystallite grain size plays a critical role in catalytic act [64]. Additionally, the decrease in crystallite size is known to have a beneficial effect on active sites dispersion, which in turn can help strengthening the co-adsorption of CO and O_2 molecules [79], and lowering the CO oxidation temperature [63,64,80]. Moreover, the structure and morphology were reported to influence the catalytic oxidation of CO [35,39]. In line with the literature studies, it could be concluded that the smallest size formed in catalyst (prepared by 5% of water) can be one of the responsible keys contributed to this highest activity against CO oxidation.

On the other hand, UV–vis measurements reveal that the optical E_g shifts towards the lower values with higher water content. This shift also guides to improve the catalytic performance in the present work. Recently, Jibril et al. reported that there is a strong correlation between the band gap energy and catalytic performance [72]. As also stated the electronic transfer occurred during the reduction-oxidation process [81], was related to the decrease in E_g allowing high electron mobility for the catalytic act. Accordingly, the synergetic effect associated with electrons transfer within the Cu_2O film may explain the observed decrease in E_g, that is in turn improves catalytic performance as also reported

by Jibril [72]. Thus, the influence of E_g on catalytic behavior demonstrates a close relationship between the optical properties of the deposited films and their catalytic performance towards CO oxidation.

To better understand the enhanced catalytic performance upon water addition, an insight on the mechanism that governs the observed catalytic behavior on the surface is of interest. It is known that the catalytic oxidation reaction of CO involves the surface oxygen species as well as the lattice oxygen if the reaction occurs at relatively high temperature, in addition to surface hydroxyls and both identified cations and anions present on the surfaces as indicated by XPS results. Thus, the oxidation reaction would be governed by the active species at the catalyst's surface. In general, the catalytic oxidation of CO over oxides follows a Mars van Krevelen mechanism involving alternate reduction and oxidation of the oxides with formation of surface oxygen vacancies and their replenishment by the adsorption and dissociation of gas phase oxygen [82,83]. This statement can be justified by XPS results which shows significant increase in surface oxygen species depending on the amount of water addition in the precursors feedstock. As results, since the ratio of lattice oxygen at surface of all the catalysts is quite equal, these surface oxygen species might exist as adsorbed oxygen as well as OH^- and oxygen vacancies on the surfaces of the catalysts. In addition, the catalyst prepared with highest water content (Cu_2O 5%) exhibited the low carbon amount (see Table S2) and therefore the highest catalytic activity towards CO oxidation, allowing appropriate accessibility to surface active sites and oxygen species.

According to White et al [17], the CO oxidation on Cu_2O surface could occur following two mechanisms: the first involves CO reaction with surface oxygen forming CO_2, yielding to oxygen vacancy creation; the second is to land on a Cu atom at the surface, then diffuse spontaneously to the neighboring surface oxygen, and produce CO_2. In addition, Le et al. [84]. studied the reactivity of Cu_2O toward CO oxidation using DFT calculations and demonstrated that the CO oxidation reaction occurs preferentially on O-terminated surfaces rather than on Cu-terminated surfaces. Furthermore, the improvement of catalytic performance obtained for doped TiO_2 support by W^{6+} was correlated to the significant enhancement of oxygen vacancies concentration as well as the modification of the electronic state of surface sites [85]. The oxygen vacancies created during the CO oxidation tend to reduce the catalytic activity of the surface. However, the surface oxygen may be restored by dissociative adsorption of gaseous oxygen presented in the reaction environment. The oxygen concentration should be high enough to enable surface oxygen recovery, and the concentration of adsorbed oxygen should not exceed the amount to avoid the surface active sites blocking [17]. In this work, the high catalytic activity of Cu_2O, prepared by water content in the feedstock, observed at even low temperatures could be tentatively explained by the contribution of the adsorbed oxygen species in the catalytic reaction, and the synergetic effect by electrons transfer within the thin Cu_2O film. The further improvement in the catalytic activity of Cu_2O 5% against CO could directly attributed to the surface oxygen species retained in the oxide films generated by the addition of the corresponding amount of water in the feedstock. Nevertheless, it was also reported that the CO oxidation reaction over metal oxides can occur without implication of surface oxygen lattice, confirming the importance role of adsorbed oxygen in the CO oxidation process [86], and as pointed out by the obtained data. Hence, these explanations demonstrate that the adsorbed oxygen species at surface of the deposit films can play an important role in the CO oxidation process.

4. Conclusions

In the present work, Cu_2O thin films were directly synthesized at low deposition temperature with PSE-CVD by considering the effect of water addition in the feedstock. All deposited films exhibited pure structure of Cu_2O and were tested in the catalytic oxidation of CO. The analysis of the crystalline structure showed that the crystallite grain size decreases with increasing the water content in the feedstock. This effect on the crystalline structure resulted in controlling the optical band gap energy of the formed films. Furthermore, these contributions improved the catalytic performance of deposited films in terms of activity towards complete CO oxidation. The variation in the adsorbed oxygen species, indicated by the XPS results, could play a significant role in the CO oxidation. All deposited films were found to be active in the total oxidation of CO at low temperature. The highest activity was observed for the sample prepared with vol. 5% of water content in the feedstock. This activity is expected to result from the adsorbed oxygen species, that are depending on the amount of water addition in the precursors feedstock. The correlation between the oxides' physicochemical properties and their catalytic activities were demonstrated. Thus, the novel approach using PSE-CVD to synthesize the transition metal oxides could open the doorway to develop catalysts for a variety of applications.

Acknowledgements

A. El Kasmi would kindly acknowledge the Deutscher Akademischer Austauschdienst (DAAD) for the financial support during his research stay at Bielefeld University, and the Moroccan National Scientific and Technique Research Center (CNRST) for his Excellency PhD Fellowship. Z.Y. Tian thanks for the financial support from the Recruitment Program of Global Youth Experts. We are grateful to Prof. K. Kohse-Höinghaus for insightful discussions and her and Prof. A. Gölzhäuser for access to their infrastructure in Bielefeld where a part of the work was performed. We also acknowledge useful discussions with Mr. M. Assebban.

Appendix A. Supplementary data

Supplementary data associated with this article can be found, in the online version, at http://dx.doi.org/10.1016/j.apcatb.2015.12.034.

References

[1] F. Oba, F. Ernst, Y. Yu, R. Liu, H.M. Kothari, J.A. Switzer, Epitaxial growth of cuprous oxide electrodeposited onto semiconductor and metal substrates, J. Am. Ceram. Soc. 88 (2005) 253–270.
[2] W.Z. Wang, G.H. Wang, X.S. Wang, Y.J. Zhan, Y.K. Liu, C.L. Zheng, Synthesis and characterization of Cu_2O nanowires by a novel reduction route, Adv. Mater. 14 (2002) 67–69.
[3] A.O. Musa, T. Akomolafe, M.J. Carter, Production of cuprous oxide, a solar cell material, by thermal oxidation and a study of its physical and electrical properties, Sol. Energy Mater. Sol. Cells 51 (1998) 305–316.
[4] R.N. Briskman, A study of electrodeposited cuprous oxide photovoltaic cells, Sol. Energy Mater. Sol. Cells 27 (1992) 361–368.
[5] C.Q. Zhang, J.P. Tu, X.H. Huang, Y.F. Yuan, X.T. Chen, F. Mao, Preparation and electrochemical performances of cubic shape Cu_2O as anode material for lithium ion batteries, J. Alloys Compd. 441 (2007) 52–56.
[6] P. Poizot, S. Laruelle, S. Grugeon, L. Dupont, J.-M. Tarascon, Nano-sized transition-metal oxides as negative-electrode materials for lithium-ion batteries, Nature 407 (2000) 496–499.
[7] S. Deng, V. Tjoa, H.M. Fan, H.R. Tan, D.C. Sayle, M. Olivo, S. Mjaisalkar, J. Wei, C.H. Sow, Reduced graphene oxide conjugated Cu_2O nanowire mesocrystals for high-performance NO_2 gas sensor, J. Am. Chem. Soc. 134 (2012) 4905–4917.
[8] J. Zhang, J. Liu, Q. Peng, X. Wang, Y. Li, Nearly monodisperse Cu_2O and CuO nanospheres: preparation and applications for sensitive gas sensors, Chem. Mater. 18 (2006) 867–871.
[9] J. Azevedo, L. Steier, P. Dias, M. Stefik, C.T. Sousa, J.P. Araújo, A. Mendes, M. Grätzel, D. Tilley, On the stability enhancement of cuprous oxide water

splitting photocathodes by low temperature steam annealing, Energy Environ. Sci. 7 (2014) 4044–4052.
[10] C. Li, T. Hisatomi, O. Watanabe, M. Nakabayashi, N. Shibata, K. Domen, J.J. Delaunay, Positive onset potential and stability of Cu_2O-based photocathodes in water splitting by atomic layer deposition of a Ga_2O_3 buffer layer, Energy Environ. Sci. 8 (2015) 1493–1500.
[11] M. Hara, T. Kondo, M. Komoda, S. Ikeda, J.N. Kondo, K. Domen, M. Hara, K. Shinohara, A. Tanaka, Cu_2O as a photocatalyst for overall water splitting under visible light irradiation, Chem. Commun. (1998) 357–358.
[12] P.E. de Jongh, D. Vanmaekelbergh, J.J. Kelly, Cu_2O: a catalyst for the photochemical decomposition of water? Chem. Commun. 106 (1999) 9–107.
[13] C.G. Morales-Guio, L. Liardet, M.T. Mayer, S.D. Tilley, M. Grätzel, X. Hu, Photoelectrochemical hydrogen production in alkaline solutions using Cu_2O coated with earth-abundant hydrogen evolution catalysts, Angew. Chem. Int. Ed. 54 (2015) 664–667.
[14] S.J.A. Moniz, S.A. Shevlin, D.J. Martin, Z.-X. Guo, J. Tang, Visible-light driven heterojunction photocatalysts for water splitting—a critical review, Energy Environ. Sci. 8 (2015) 731–759.
[15] G. Yuan, J. Zhu, F. Xie, X. Chang, Shape-controlled synthesis of cuprous oxide nanocrystals via the electrochemical route with H_2O-polyol mix-solvent and their behaviors of adsorption, J. Nanosci. Nanotechnol. 10 (2010) 5258–5264.
[16] J. Ramírez-Ortiz, T. Ogura, J. Medina-Valtierra, S.E. Acosta-Ortiz, P. Bosch, J. Antonio de los Reyes, V.H. Lara, A catalytic application of Cu_2O and CuO films deposited over fiberglass, Appl. Surf. Sci. 174 (2001) 177–184.
[17] B. White, M. Yin, A. Hall, D. Le, S. Stolbov, T. Rahman, N. Turro, S. O'Brien, Complete CO oxidation over Cu_2O nanoparticles supported on silica gel, Nano Lett. 6 (2006) 2095–2098.
[18] V. Figueiredo, E. Elangovan, G. Gonçalves, N. Franco, E. Alves, S.H.K. Park, R. Martins, E. Fortunato, Electrical, structural and optical characterization of copper oxide thin films as a function of post annealing temperature, Phys. Status Solidi A 206 (2009) 2143–2148.
[19] T. Kosugi, S. Kaneko, Novel spray-pyrolysis deposition of cuprous oxide thin films, J. Am. Ceram. Soc. 81 (1998) 3117–3124.
[20] M. Wei, J. Huo, Preparation of Cu_2O nanorods by a simple solvothermal method, Mater. Chem. Phys. 121 (2010) 291–294.
[21] L. Gou, C.J. Murphy, Solution-phase synthesis of Cu_2O nanocubes, Nano Lett. 3 (2002) 231–234.
[22] M. Salavati-Niasari, F. Davar, Synthesis of copper and copper(I) oxide nanoparticles by thermal decomposition of a new precursorhesis of copper and copper(I) oxide nanoparticles by thermal decomposition of a new precursor, Mater. Lett. 63 (2009) 441–443.
[23] Y. Gu, X. Su, Y. Du, C. Wang, Preparation of flower-like Cu_2O nanoparticles by pulse electrodeposition and their electrocatalytic application, Appl. Surf. Sci. 256 (2010) 5862–5866.
[24] S.C. Ray, Preparation of copper oxide thin film by the sol–gel-like dip technique and study of their structural and optical properties, Sol. Energy Mater. Sol. Cells 68 (2001) 307–312.
[25] H. Zhu, J. Zhang, C. Li, F. Pan, T. Wang, B. Huang, Cu_2O thin films deposited by reactive direct current magnetron sputtering, Thin Solid Films 517 (2009) 5700–5704.
[26] C. Du, M. Xiao, Cu_2O nanoparticles synthesis by microplasma, Sci. Rep. 4 (2014) 7339.
[27] M.D. Susman, Y. Feldman, A. Vaskevich, I. Rubinstein, Chemical deposition of Cu_2O nanocrystals with precise morphology control, ACS Nano 8 (2014) 162–174.
[28] G.F. Pan, S.B. Fan, J. Liang, Y.X. Liu, Z.Y. Tian, CVD synthesis of Cu_2O films for catalytic application, RSC Adv. 5 (2015) 42477–42481.
[29] M. Ristov, G. Sinadinovski, I. Grozdanov, Chemical deposition of Cu_2O thin films, Thin Solid Films 123 (1985) 63–67.
[30] Z.Y. Tian, H.J. Herrenbrück, P.M. Kouotou, H. Vieker, A. Beyer, A. Gölzhäuser, K. Kohse-Höinghaus, Facile synthesis of catalytically active copper oxide from pulsed-spray evaporation CVD, Surf. Coat. Technol. 230 (2013) 33–38.
[31] Z. Wang, H. Wang, L. Wang, L. Pan, Controlled synthesis of Cu_2O cubic and octahedral nano- and microcrystals, Cryst. Res. Technol. 44 (2009) 624–628.
[32] M. Cao, C. Hu, Y. Wang, Y. Guo, C. Guo, E. Wang, A controllable synthetic route to Cu, Cu_2O, and CuO nanotubes and nanorods, Chem. Commun. 188 (2003) 1884–1885.
[33] N. Bahlawane, P.A. Premkumar, Z.Y. Tian, X. Hong, F. Qi, K. Kohse-Höinghaus, Nickel and nickel-based nanoalloy thin films from alcohol-assisted chemical vapor deposition, Chem. Mater. 22 (2009) 92–100.
[34] P.A. Premkumar, N.S. Prakash, F. Gaillard, N. Bahlawane, CVD of Ru, Pt and Pt-based alloy thin films using ethanol as mild reducing agent, Mater. Chem. Phys. 125 (2011) 757–762.
[35] P.M. Kouotou, H. Vieker, Z.Y. Tian, P.H. Tchoua Ngamou, A. El Kasmi, A. Beyer, A. Gölzhäuser, K. Kohse-Höinghaus, Structure–activity relation of spinel-type Co–Fe oxides for low-temperature CO oxidation, Catal. Sci. Technol. 4 (2014) 3359–3367.
[36] P.M. Kouotou, Z.Y. Tian, H. Vieker, K. Kohse-Höinghaus, Pulsed-spray evaporation CVD synthesis of hematite thin films for catalytic conversion of CO, Surf. Coat. Technol. 230 (2013) 59–65.
[37] Z.Y. Tian, P.M. Kouotou, N. Bahlawane, P.H. Tchoua Ngamou, Synthesis of the catalytically active Mn_3O_4 spinel and its thermal properties, J. Phys. Chem. C 117 (2013) 6218–6224.
[38] Z.Y. Tian, P.H. Tchoua Ngamou, V. Vannier, K. Kohse-Höinghaus, N. Bahlawane, Catalytic oxidation of VOCs over mixed Co–Mn oxides, Appl. Catal. B: Environ. 117–118 (2012) 125–134.
[39] Z.Y. Tian, H. Vieker, P.M. Kouotou, A. Beyer, In situ characterization of Cu–Co oxides for catalytic application, Faraday Discuss. 177 (2015) 249–262.
[40] Z.Y. Tian, P.M. Kouotou, A. El Kasmi, P.H. Tchoua Ngamou, K. Kohse-Höinghaus, H. Vieker, A. Beyer, A. Gölzhäuser, Low-temperature deep oxidation of olefins and DME over cobalt ferrite, Proc. Combust. Inst. 35 (2015) 2207–2214.
[41] S. Royer, D. Duprez, Catalytic oxidation of carbon monoxide over transition metal oxides, ChemCatChem 3 (2011) 24–65.
[42] J. Qi, J. Chen, G. Li, S. Li, Y. Gao, Z. Tang, Facile synthesis of core–shell Au@CeO_2 nanocomposites with remarkably enhanced catalytic activity for CO oxidation, Energy Environ. Sci. 5 (2012) 8937–8941.
[43] D.J. Little, M.R. Smith III, T.W. Hamann, Electrolysis of liquid ammonia for hydrogen generation, Energy Environ. Sci. 8 (2015) 2775–2781.
[44] D.A. Hickman, L.D. Schmidt, Production of syngas by direct catalytic oxidation of methane, Science 259 (1993) 343–346.
[45] J.B. Joo, M. Dahl, N. Li, F. Zaera, Y. Yin, Tailored synthesis of mesoporous TiO_2 hollow nanostructures for catalytic applications, Energy Environ. Sci. 6 (2013) 2082–2092.
[46] Z. Qi, C. He, A. Kaufman, Effect of CO in the anode fuel on the performance of PEM fuel cell cathode, J. Power Sour. 111 (2002) 239–247.
[47] M. Watanabe, H. Uchida, K. Ohkubo, H. Igarashi, Hydrogen purification for fuel cells: selective oxidation of carbon monoxide on Pt–Fe/zeolite catalysts, Appl. Catal. B: Environ. 46 (2003) 595–600.
[48] X. Xie, Y. Li, Z.-Q. Liu, M. Haruta, W. Shen, Low-temperature oxidation of CO catalysed by Co_3O_4 nanorods, Nature 458 (2009) 746–749.
[49] M.V. Twigg, Progress and future challenges in controlling automotive exhaust gas emissions, Appl. Catal. B: Environ. 70 (2007) 2–15.
[50] X. Chen, Y. Cheng, C.Y. Seo, J.W. Schwank, R.W. McCabe, Aging re-dispersion, and catalytic oxidation characteristics of model Pd/Al_2O_3 automotive three-way catalysts, Appl. Catal. B: Environ. 163 (2015) 499–509.
[51] C.T. Campbell, G. Ertl, H. Kuipers, J. Segner, A molecular beam study of the catalytic oxidation of CO on a Pt(1 1 1) surfacelecular beam study of the catalytic oxidation of CO on a Pt(1 1 1) surface, J. Chem. Phys. 73 (1980) 5862–5873.
[52] D. Widmann, R.J. Behm, Active oxygen on a Au/TiO_2 Catalyst: formation, stability, and CO oxidation activity, Angew. Chem. Int. Ed. 50 (2011) 10241–10245.
[53] I.X. Green, W. Tang, M. Neurock, J.T. Yates, Spectroscopic observation of dual catalytic sites during oxidation of CO on a Au/TiO_2 catalyst, Science 333 (2011) 736–739.
[54] K. An, S. Alayoglu, N. Musselwhite, S. Plamthottam, G. Melaet, A.E. Lindeman, G.A. Somorjai, Enhanced CO oxidation rates at the interface of mesoporous oxides and Pt nanoparticles, J. Am. Chem. Soc. 135 (2013) 16689–16696.
[55] Y. Guo, D. Gu, Z. Jin, P.-P. Du, R. Si, J. Tao, W.Q. Xu, Y.Y. Huang, S. Senanayake, Q.S. Song, C.J. Jia, F. Schüth, Uniform 2 nm gold nanoparticles supported on iron oxides as active catalysts for CO oxidation reaction: structure–activity relationship, Nanoscale 7 (2015) 4920–4928.
[56] T. Fujitani, I. Nakamura, Mechanism and active sites of the oxidation of CO over Au/TiO_2, Angew. Chem. Int. Ed. 50 (2011) 10144–10147.
[57] P. Sudarsanam, B. Mallesham, P.S. Reddy, D. Großmann, W. Grünert, B.M. Reddy, Nano-Au/CeO2 catalysts for CO oxidation: influence of dopants (Fe, La and Zr) on the physicochemical properties and catalytic activity, Appl. Catal. B: Environ. 144 (2014) 900–908.
[58] N. Bahlawane, P.H. Tchoua Ngamou, V. Vannier, T. Kottke, J. Heberle, K. Kohse-Höinghaus, Tailoring the properties and the reactivity of the spinel cobalt oxide, Phys. Chem. Chem. Phys. 11 (2009) 9224–9232.
[59] A.-P. Jia, G.-S. Hu, L. Meng, Y.-L. Xie, J.-Q. Lu, M.-F. Luo, CO oxidation over CuO/$Ce_{1-x}CuxO_{2-\delta}$ and $Ce_{1-x}CuxO_{2-\delta}$ catalysts: synergetic effects and kinetic study, J.Catal. 289 (2012) 199–209.
[60] K. Huang, X. Chu, L. Yuan, W. Feng, X. Wu, X. Wang, S. Feng, Engineering the surface of perovskite $La_{0.5}Sr_{0.5}MnO_3$ for catalytic activity of CO oxidation, Chem. Commun. 50 (2014) 9200–9203.
[61] T. Biemelt, K. Wegner, J. Teichert, S. Kaskel, Microemulsion flame pyrolysis for hopcalite nanoparticle synthesis: a new concept for catalyst preparation, Chem. Commun. 51 (2015) 5872–5875.
[62] Z.Y. Tian, N. Bahlawane, F. Qi, K. Kohse-Höinghaus, Catalytic oxidation of hydrocarbons over Co_3O_4 catalyst prepared by CVD, Catal. Commun. 11 (2009) 118–122.
[63] M. Jin, H. Liu, H. Zhang, Z. Xie, J. Liu, Y. Xia, Synthesis of Pd nanocrystals enclosed by {1 0 0} facets and with sizes <10 nm for application in CO oxidation, Nano Res. 4 (2010) 83–91.
[64] N. Uekawa, M. Ueta, Y.J. Wu, K. Kakegawa, Synthesis of CeO_2 spherical fine particles by homogeneous precipitation method with polyethylene glycol, Chem. Lett. 85 (2002) 854–855.
[65] K. Qadir, S.H. Joo, B.S. Mun, D.R. Butcher, J.R. Renzas, F. Aksoy, Z. Liu, G.A. Somorjai, J.Y. Park, Intrinsic relation between catalytic activity of CO oxidation on Ru nanoparticles and Ru oxides uncovered with ambient pressure XPS, Nano Lett. 12 (2012) 5761–5768.
[66] B.W. Ward, J.A. Notte, N.P. Economou, Helium ion microscope: A new tool for nanoscale microscopy and metrology, J. Vac. Sci. Technol. B 24 (2006) 2871–2874.
[67] C.-H. Kuo, C.-H. Chen, M.H. Huang, Seed-mediated synthesis of monodispersed Cu_2O nanocubes with five different size ranges from 40 to 420 nm, Adv. Funct. Mater. 17 (2007) 3773–3780.
[68] M.C. Biesinger, L.W.M. Lau, A.R. Gerson, R.S.C. Smart, Resolving surface chemical states in XPS analysis of first row transition metals, oxides and hydroxides: Sc, Ti, V, Cu and Zn, Appl. Surf. Sci. 257 (2010) 887–898.

[69] C.J.A. Powell Jablonski, NIST Electron Effective- Attenuation-length Database—Version 1.3, National Institute of Standard s and Technology, Gaithersburg, 2011.
[70] J. Pinkas, J.C. Huffman, D.V. Baxter, M.H. Chisholm, K.G. Caulton, Mechanistic role of H_2O and the ligand in the chemical vapor deposition of Cu, Cu_2O CuO, and Cu_3N from Bis(1, 1,1,5,5,5-hexafluoropentane-2,4-dionato) copper(II), Chem. Mater. 7 (1995) 1589–1596.
[71] Z.Y. Tian, N. Bahlawane, V. Vannier, K. Kohse-Höinghaus, Structure sensitivity of propene oxidation over Co-Mn spinels, Proc. Combust. Inst. 34 (2013) 2261–2268.
[72] B.Y. Jibril, Catalytic performances and correlations with metal oxide band gaps of metal-tungsten mixed oxide catalysts in propane oxydehydrogenation, React. Kinet. Catal. Lett. 86 (2005) 171–177.
[73] V. Georgieva, M. Ristov, Electrodeposited cuprous oxide on indium tin oxide for solar applications, Sol. Energy Mater. Sol. Cells 73 (2002) 67–73.
[74] M.Y. Shen, T. Yokouchi, S. Koyama, T. Goto, Dynamics associated with Bose-Einstein statistics of orthoexcitons generated by resonant excitations in cuprous oxide, Phys. Rev. B 56 (1997) 13066–13072.
[75] J. Ghijsen, L.H. Tjeng, J. van Elp, H. Eskes, J. Westerink, G.A. Sawatzky, M.T. Czyzyk, Electronic structure of Cu_2O and CuO, Phys. Rev. B 38 (1988) 11322–11330.
[76] F.K. Mugwang'a, P.K. Karimi, W.K. Njoroge, O. Omayio, S.M. Waita, Optical characterization of copper oxide thin films prepared by reactive dc magnetron sputtering for solar cell applications, Int. J. Adv. Renew. Energy Res. 1 (2012) 58 http://www.grscitechpress.org/index.php/IJARER/article/view/.
[77] A. Bielański, J. Haber, Oxygen in catalysis on transition metal oxides, Catal. Rev. 19 (1979) 1–41.
[78] Y.S. Chaudhary, A. Agrawal, R. Shrivastav, V.R. Satsangi, S. Dass, A study on the photoelectrochemical properties of copper oxide thin films, Int. J. Hydrog. Energy. 29 (2004) 131–134.
[79] Y. Gao, N. Shao, Y. Pei, Z. Chen, X.C. Zeng, Catalytic activities of subnanometer gold clusters (Au16–Au18, Au20, and Au27–Au35) for CO oxidation, ACS Nano 5 (2011) 7818–7829.
[80] M.-F. Luo, Z.-Y. Hou, X.-X. Yuan, X.-M. Zheng, Characterization study of CeO_2 supported Pd catalyst for low-temperature carbon monoxide oxidation, Catal. Lett. 50 (1998) 205–209.
[81] P.J. Gellings, H.J.M. Bouwmeester, Ion and mixed conducting oxides as catalysts, Catal. Today 12 (1992) 1–101.
[82] H. Bao, X. Chen, J. Fang, Z. Jiang, W. Huang, Structure-activity relation of Fe_2O_3–CeO_2 composite catalysts in CO oxidation, Catal. Lett. 125 (2008) 160–167.
[83] E. Aneggi, J. Llorca, M. Boaro, A. Trovarelli, Surface-structure sensitivity of CO oxidation over polycrystalline ceria powders, J. Catal. 234 (2005) 88–95.
[84] D. Le, S. Stolbov, T.S. Rahman, Reactivity of the Cu_2O (1 0 0) surface: insights from first principles calculations, Surf. Sci. 603 (2009) 1637–1645.
[85] T. Chafik, A.M. Efstathiou, X.E. Verykios, Effects of W^{6+} doping of TiO_2 on the reactivity of supported Rh toward NO: Transient FTIR and mass spectroscopy studies, J. Phys. Chem. B 101 (1997) 7968–7977.
[86] W. Yang, R. Zhang, B. Chen, N. Bion, D. Duprez, S. Royer, Activity of perovskite-type mixed oxides for the low-temperature CO oxidation: Evidence of oxygen species participation from the solid, J. Catal. 295 (2012) 45–58.